Uncertainty quantification for human arterial network

Peng Chen[1] **Alfio Quarteroni**[1,2] **Gianluigi Rozza**[1]

CMCS - MATHICSE - EPFL, Switzerland [1] MOX - Politecnico di Milano, Italy [2]

peng.chen@epfl.ch, alfio.quarteroni@epfl.ch, gianluigi.rozza@epfl.ch

Abstract: This work deals with identifying and quantifying uncertainties from various sources in a relatively complete human arterial network that is validated against clinical measurements for the first time. We establish a stochastic multiscale system consisting of one dimensional fluid structure interaction model (FSI) and zero dimensional lumped parameter model to describe the pulse wave propagation of blood flow and pressure. Distinct uncertainty effect is studied through statistics and sensitivity of the solution with respect to many different parametric uncertainties.

Uncertainties in Arterial Network

We investigate diverse uncertainties in the human arterial network with schematic representation in Figure 1.

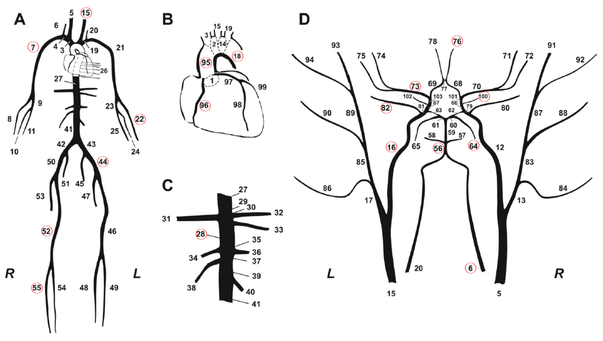

Figure 1: *Representation of the human arterial network [1]*

In general, they can be classified as ***1. Computational geometries:*** e.g. cross section area in lumen, wall thickness, image noise; ***2. Mathematical models:*** e.g. rigid or compliant walls, with or without viscoelastic or inertial properties; ***3. Physical parameters:*** e.g. Young's modulus, characteristic time, the density, diffusivity; ***4. Boundary conditions:*** e.g. inlet velocities or flux, outlet resistance, compliance; ***5. External sources or forces:*** e.g. external pressure from surrounding tissue, work efforts.

These uncertainties can be represented in the probability framework and calibrated from measurements through regression, maximum likelihood estimation, maximum entropy and other inference techniques. In the absence of sufficient data, we use a parametric uncertainty form with lognormal distribution that is positive and concentrated

$$\eta(t,x,\omega) = \exp\big(\mu_e + \sigma_v Y(\omega)\big)\eta(t,x) \tag{1}$$

with different (μ_e, σ_v) for different degrees of uncertainties. Figure 2 depicts the standard normal distribution function of Y and several lognormal distribution functions.

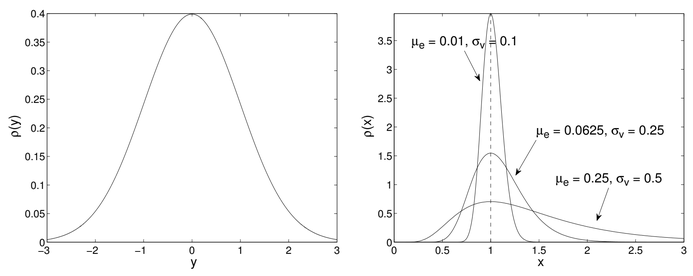

Figure 2: *Normal, lognormal probability density functions with noise-to signal ratio around* $10\%, 25\%, 50\%$*, respectively*

Stochastic Multiscale Model

We consider the following elements in building the stochastic multiscale model to describe uncertainty effect for wave propagation of blood flow and pressure in arterial network.

- ***FSI: reduced from 3D to 1D in large scale***

  By integrating the 3D Navier-Stokes equations over the cross section, we obtain the reduced 1D fluid equations with state variables $(A, Q, P) : (0,T] \times [0,L] \times \Omega \to \mathbb{R}^3$ [2]

$$\begin{cases} \dfrac{\partial A}{\partial t} + \dfrac{\partial Q}{\partial x} = 0, \\ \dfrac{\partial Q}{\partial t} + \dfrac{\partial}{\partial x}\left(\alpha \dfrac{Q^2}{A}\right) + \dfrac{A}{\rho}\dfrac{\partial P}{\partial x} + k(\mu)\dfrac{Q}{A} = 0, \end{cases} \tag{2}$$

  which is closed with the pressure-area relation

$$P - P_{ext} = \psi_\beta(A_0, A, E) + \psi_\gamma(A_0, A, \partial_t A, T), \tag{3}$$

  being P_{ext} external pressure, ψ_β, ψ_γ elastic and viscoelastic terms, A_0 reference area, E Young modulus and T characteristic time accounting for material properties.

- ***0D lumped parameter model in small scale***

  The lumped parameter model with analogy to electrical network is applied to describe blood flow in small scale:

$$P - P_v + CR_2\frac{dP}{dt} = RQ + CR_1R_2\frac{dQ}{dt}, \tag{4}$$

  where P_v is venous pressure, C and $R = R_1 + R_2$ are compliance and resistance with assumption $R_1 = 4R_2$.

- ***Domain decomposition at the bifurcation***

  Conservation of mass the continuity of pressure lead to

$$\sum_{n=1}^{N_p} Q_n^p = \sum_{m=1}^{N_d} Q_m^d, \quad \text{and} \quad P_n^p = P_m^d, \tag{5}$$

  at each bifurcation for proximal and distal state variables (Q_n^p, P_n^p) and (Q_m^d, P_m^d), $\forall\, n = 1, \ldots, N_p, m = 1, \ldots, N_d$.

- ***Stochastic multiscale arterial network model***

  The complete model for the arterial network presented in Figure 1 is constructed by coupling the equations (2) and (3) for each large scale arterial segment , equation (4) for each small scale terminal network feeding boundary conditions, equation (5) for wave propagation at each bifurcation, as well as some prescribed physiological flow rate Q at the heart and suitable initial conditions, e.g. $A = A_0, Q = 0, P = P_{ext}$, for the entire arterial network. All the uncertainties in red are parametrized via (1).

Approximation & Simulation

We specify numerical approximation of the stochastic multiscale model and computational strategy for simulation as:

- ***Deterministic approximation in physical space***

  We split the flow rate and thus the model into the **(a)** elastic and **(b)** viscoelastic parts for simplicity, and then solve the FSI problem in two steps by second order Taylor Galerkin approach using nonlinear Richardson scheme and Broyden algorithm for updating Jacobian matrix [3].

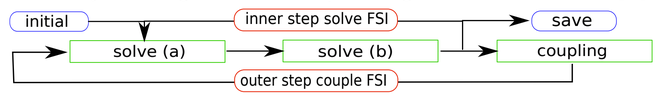

- ***Stochastic approximation in probability space***

  We use the non-intrusive spare grid stochastic collocation method for approximation in probability space [4]

$$\mathcal{S}_q f(y) = \sum_{q-K+1 \le |i| \le q} (-1)^{q-|i|} \binom{K-1}{q-|i|} \left(\mathcal{U}^{i_1} \otimes \cdots \otimes \mathcal{U}^{i_K}\right) f(y), \tag{6}$$

  where $|i| = \sum i_k$ with the multivariate index $i = (i_1, \ldots, i_K)$ defined via various sets, e.g. type I ($|i| \le w$) and II ($\prod i_k \le w$) in Figure 3.

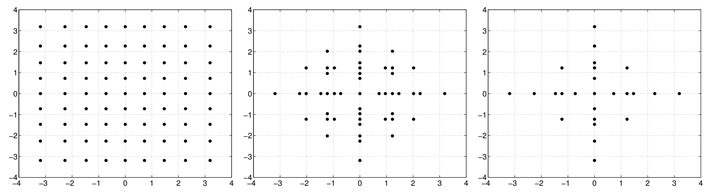

Figure 3: *Tensor product grid and sparse grid of type I & II*

The statistics (mean $\mathbb{E}$, standard deviation $\mathbb{S} = \sqrt{\mathbb{V}}$) and sensitivity (main effect $\mathbb{G}_k, 1 \le k \le K$) is evaluated as [2]

$$\mathbb{E}[f] \approx \int_\Gamma \mathcal{S}_q f(y)\rho(y)dy;\ \mathbb{V}[f] \approx \mathbb{E}\left[\mathcal{S}_q f^2\right] - \left(\mathbb{E}[\mathcal{S}_q f]\right)^2;\ \mathbb{G}_k[f] = \frac{\mathbb{V}[\mathbb{E}[f|y_k]]}{\mathbb{V}[f]}$$

- ***Simulation: two level parallel computation in LifeV***

  Due to the non-intrusive property of collocation approach, we parallelize the simulation in N stochastic groups in the 1st level and use M processors for each deterministic solver in the 2nd level. In practice, we use 10×16 processors, i.e. 16 processors (Intel Xeon Nehalem 2.66 GHz, costing 25 minutes) for each of 10 deterministic solvers at 10 collocation nodes for a period of 6 heart beats.

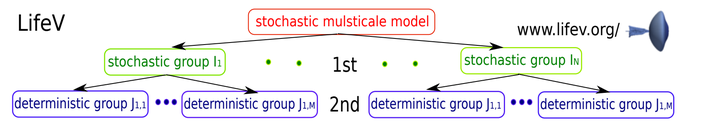

Experiments in 1 dimension

We impose physiological flow rate at Ascending aorta 1 and randomize it with 10% noise, with results shown in Figure 4

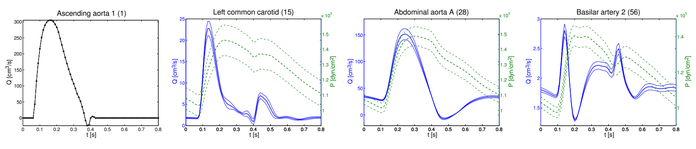

Figure 4: *Prescribed inflow rate* Q *and the statistics* $\mathbb{E}, \mathbb{E}+\mathbb{S}, \mathbb{E}-\mathbb{S}$

To explore the convergence property of the stochastic collocation method, we define the relative error for $\mathbb{E}$ and $\mathbb{S}$ as

$$\text{error}(\mathbb{E}_l[f]) = \frac{||\mathbb{E}[\mathcal{S}_{q+1}f] - \mathbb{E}[\mathcal{S}_q f]||}{||\mathbb{E}[\mathcal{S}_{q+1}f]||};\ \text{error}(\mathbb{S}_l[f]) = \frac{||\mathbb{S}[\mathcal{S}_{q+1}f] - \mathbb{S}[\mathcal{S}_q f]||}{||\mathbb{S}[\mathcal{S}_{q+1}f]||},$$

We consider noise $10\%, 25\%, 50\%$ (see Figure 2) for reference area A_0, resistance R and Young modulus E, respectively, and use different collocation level $l = q - K$, with pressure shown at 18 representative locations in Figure 5

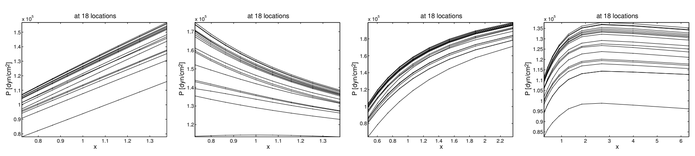

Figure 5: *Pressure at 18 representative locations for* Q*,*A_0*,*R *and* E

The a posteriori relative error (value in $\times 10^{-3}$) is displayed in Table 1, from which we can see that nonlinear relation with large noise (e.g. E) needs high level of interpolation.

parameter	inflow rate Q		area A_0		resistance R			Young modulus E		
level l	1	2	1	2	1	2	3	1	2	3
error($\mathbb{E}_l[Q]$)	0.012	0.008	0.078	0.048	0.013	0.011	0.007	11.687	3.186	0.422
error($\mathbb{S}_l[Q]$)	0.317	0.236	3.218	2.356	1.469	0.226	0.165	92.540	39.088	8.959
error($\mathbb{E}_l[P]$)	0.003	0.002	0.011	0.007	0.003	0.003	0.002	1.677	0.492	0.075
error($\mathbb{S}_l[P]$)	0.068	0.051	0.656	0.438	0.082	0.025	0.020	42.766	15.812	2.565

Table 1: *A posteriori error of the statistics of* (Q, A_0, R, E) *in different levels* ($\times 10^{-3}$)

Experiments in 10 dimensions

We examine systematically 10 parameters for their impact via main effect $\mathbb{G}_k, 1 \le k \le 10$, see Table 2 and Figure 6

location/parameter	ρ	μ	P_v	P_{ext}	Q	R	C	T	E	A_0
Ascending aorta 2	0.086	0.046	6.496	0.070	62.034	21.776	0.007	0.001	1.296	6.661
Left common carotid	0.083	0.046	6.845	0.068	62.171	21.443	0.007	0.000	1.232	6.479
Left radial	0.048	0.072	5.649	0.087	61.563	28.581	0.008	0.000	0.964	1.124
Abdominal aorta A	0.063	0.044	6.817	0.071	62.062	22.567	0.007	0.000	1.180	5.544
Right anterior tibial	0.892	0.111	4.641	0.125	52.807	36.620	0.006	0.001	0.838	1.484
Right post. cerebral 2	0.146	0.066	7.104	0.110	59.873	28.980	0.007	0.001	0.907	0.181
Basilar artery 2	0.001	0.057	6.483	0.101	62.221	25.149	0.007	0.001	1.083	3.080
Right vertebral	0.041	0.048	7.000	0.078	62.399	22.382	0.007	0.000	1.140	5.158
Left ophthalmic	0.116	0.076	8.085	0.055	60.976	26.420	0.006	0.001	0.905	0.420

Table 2: *Sensitivity analysis: sensitivity* $\mathbb{G}_k$ *of different parameters to pressure* P *at 18 locations (%)*

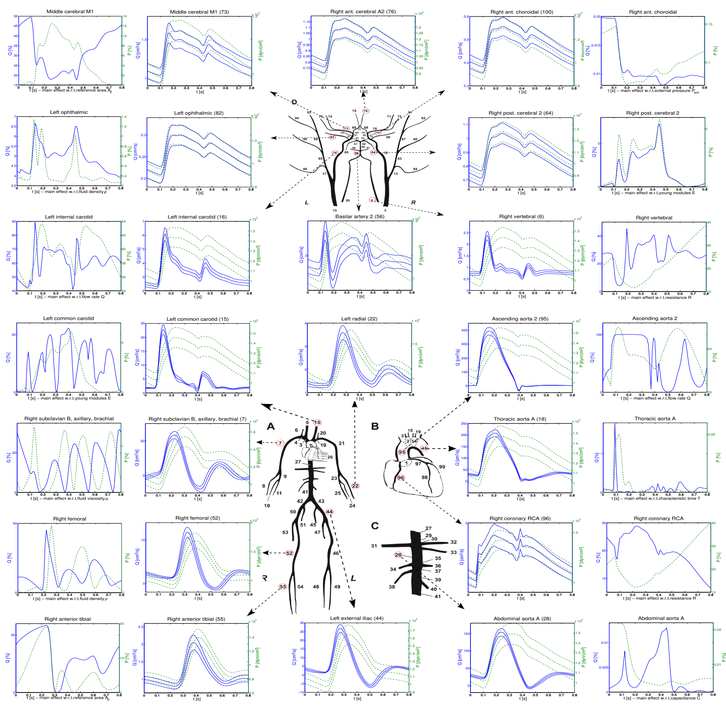

Figure 6: *Time dependent statistics and sensitivity at 18 locations*

Experiments in 103 dimensions

We assume that the reference area A_0 at each segment is randomized with i.i.d. $Y_m \sim \mathcal{N}(0,1)$ and $\mu_e = 0.01, \sigma_v = 0.1$

$$A_0^m(x,\omega) = \exp(\mu_e + \sigma_v Y_m(\omega))A_0(x), 1 \le m \le 103,$$

With small noise (10%), we use the first level of interpolation to evaluate the sensitivity, with results for flow rate and pressure displayed in Table 3 and 4 respectively, from which we conclude that the influential uncertainties come from the nearest segments for Q, while near heart (e.g. 27,95) for P.

location/order	1st	2nd	3rd	4th	5th	1-5
Ascending aorta 2 (95)	77.616 (95)	7.039 (1)	5.138 (98)	1.907 (27)	1.225 (46)	92.925
Left common carotid (15)	58.289 (16)	10.457 (12)	7.408 (15)	3.479 (69)	3.311 (68)	82.943
Left radial (22)	89.126 (22)	2.912 (21)	2.443 (27)	1.362 (95)	0.994 (7)	96.837
Abdominal aorta A (28)	15.811 (95)	10.886 (7)	10.786 (21)	8.570 (52)	8.570 (46)	54.623
Right anterior tibial (55)	92.292 (55)	6.218 (52)	0.329 (54)	0.318 (95)	0.181 (7)	99.338
Right post. cerebral 2 (64)	91.862 (64)	1.878 (27)	1.287 (95)	0.743 (21)	0.670 (18)	96.441
Basilar artery 2 (56)	27.970 (9)	18.040 (20)	15.745 (16)	15.338 (6)	15.088 (12)	92.181
Right vertebral (6)	63.532 (6)	19.705 (20)	6.048 (9)	3.454 (16)	3.319 (12)	96.058
Left ophthalmic (82)	98.458 (82)	0.491 (16)	0.267 (27)	0.180 (95)	0.096 (9)	99.492

Table 3: *The largest five values and their summation of main effect (value in percent (%)) of* Q *with respect to reference area from their corresponding boundaries in bracket* $(\cdot)$ *at 10 locations*

location/order	1st	2nd	3rd	4th	5th	1-5
Ascending aorta 2 (95)	24.309 (27)	16.979 (95)	8.655 (18)	7.586 (21)	7.217 (7)	64.745
Left common carotid (15)	24.982 (27)	16.981 (95)	8.859 (18)	7.841 (21)	7.411 (7)	66.074
Left radial (22)	44.965 (22)	13.821 (21)	12.215 (27)	7.231 (95)	3.974 (7)	82.208
Abdominal aorta A (28)	22.207 (95)	10.407 (21)	9.691 (7)	8.295 (18)	8.071 (9)	58.672
Right anterior tibial (55)	50.087 (55)	40.073 (52)	2.088 (95)	2.007 (54)	1.093 (7)	95.347
Right post. cerebral 2 (64)	63.271 (64)	8.232 (27)	5.648 (95)	3.260 (21)	2.936 (18)	83.346
Basilar artery 2 (56)	21.416 (27)	14.728 (95)	8.760 (21)	7.740 (7)	7.629 (18)	60.272
Right vertebral (6)	23.829 (27)	16.475 (95)	10.724 (7)	8.473 (18)	8.384 (21)	67.885
Left ophthalmic (82)	62.446 (82)	11.727 (16)	6.309 (27)	4.281 (95)	2.287 (9)	87.050

Table 4: *The largest five values and their summation of main effect (value in percent (%)) of* P *with respect to reference area from their corresponding boundaries in bracket* $(\cdot)$ *at 10 locations*

References

[1] P. Reymond, F. Merenda, F. Perren, D. Rufenacht and N. Stergiopulos. Validation of a one-dimensional model of the systemic arterial tree, AJPHCP, 2009.

[2] P. Chen, A. Quarteroni, G. Rozza, Systematic uncertainty quantification of a one-dimensional human arterial network. submitted, 2012

[3] A.C.I. Malossi, P.J. Blanco, and S. Deparis. A two-level time step technique for the partitioned solution of one-dimensional arterial networks. CMAME, 2012.

[4] I. Babuska, F. Nobile, and R. Tempone. A stochastic collocation method for elliptic partial differential equations with random input data. SIAM review,2010.

[5] D. Xiu and S.J. Sherwin. Parametric uncertainty analysis of pulse wave propagation in a model of a human arterial network. JCP, 2007.

Conclusion: The uncertainty quantification strategy we presented is helpful to detect systematically and quantitatively the importance of various parameters to human arterial network.